SAP-Bench: Benchmarking Multimodal Large Language Models in Surgical Action Planning

Mengya Xu[1,*], Zhongzhen Huang[2,*], Dillan Imans[3], Yiru Ye[4], Xiaofan Zhang[2,†], Qi Dou[1,†]
[1] The Chinese University of Hong Kong, Hong Kong SAR, China
[2] Shanghai Jiao Tong University, Shanghai, China
[3] Sungkyunkwan University, Seoul, South Korea
[4] The First Affiliated Hospital of Wenzhou Medical University, Wenzhou, China
[*] Equal contribution [†] Corresponding author

Abstract

Effective evaluation is critical for driving advancements in MLLM research. The surgical action planning (SAP) task, which aims to generate future action sequences from visual inputs, demands precise and sophisticated analytical capabilities. Unlike mathematical reasoning, surgical decision-making operates in life-critical domains and requires meticulous, verifiable processes to ensure reliability and patient safety. This task demands the ability to distinguish between atomic visual actions and coordinate complex, long-horizon procedures, capabilities that are inadequately evaluated by current benchmarks. To address this gap, we introduce SAP-Bench, a large-scale, high-quality dataset designed to enable multimodal large language models (MLLMs) to perform interpretable surgical action planning. Our SAP-Bench benchmark, derived from the cholecystectomy procedures context with the mean duration of $1137.5s$, and introduces temporally-grounded surgical action annotations, comprising the $1,226$ clinically validated action clips (mean duration: $68.7s$) capturing five fundamental surgical actions across 74 procedures. The dataset provides $1,152$ strategically sampled *current frames*, each paired with the corresponding *next action* as multimodal analysis anchors. We propose the MLLM-SAP framework that leverages MLLMs to generate *next action* recommendations from the current surgical scene and natural language instructions, enhanced with injected surgical domain knowledge. To assess our dataset's effectiveness and the broader capabilities of current models, we evaluate seven state-of-the-art MLLMs (e.g., OpenAI-o1, GPT-4o, QwenVL2.5-72B, Claude-3.5-Sonnet, GeminiPro2.5, Step-1o, and GLM-4v) and reveal critical gaps in *next action* prediction performance. The dataset is available at `https://huggingface.co/datasets/SAPbench/SAPBench`.

1 Introduction

The growing complexity of artificial intelligence applications has revealed the limitations of unimodal data processing, shifting research attention toward multimodal reasoning models. Although multimodal large language models (MLLMs) have achieved significant progress in vision-language tasks (e.g., image captioning, visual question answering), current approaches still face challenges in handling intricate multimodal tasks, adapting to dynamic and open environments, and achieving human-like comprehensive perception and deep reasoning. As the capabilities of MLLMs continue to advance, there is an increasing need for high-quality, comprehensive datasets that can more effectively evaluate their performance.

A robust benchmarking framework not only quantifies model performance but also reveals key strengths and weaknesses. For example, [7] demonstrates that while modern MLLMs exhibit

Preprint. Under review.

strong holistic image understanding, their ability to reason about localized regions remains limited. Additionally, [14] highlights challenges in fine-grained relational reasoning, suggesting room for improvement in detailed scene comprehension. The continued progress of MLLMs hinges on developing more rigorous and systematic evaluation frameworks. As these models grow in sophistication, they demand increasingly nuanced and high-quality benchmarks to accurately measure their capabilities. This symbiotic interplay, where advancements in MLLMs drive the need for better evaluation, and improved evaluation in turn fosters model development, mirrors an iterative refinement process, propelling the field forward.

While existing benchmarks have advanced multimodal understanding in general domains (e.g., MMMU [26], ScienceQA [17]), they lack the surgical specificity needed to evaluate clinical decision-making. Similarly, medical benchmarks (e.g., MedQA, radiology datasets) remain constrained by either single-modality analysis (text or images alone) or passive question-answering formats, failing to capture the proactive, sequential reasoning required for surgical action planning. This leaves a critical gap in assessing how multimodal models integrate diverse data sources, including temporal visual cues, procedural text, and surgical domain knowledge, to support dynamic clinical decisions.

Surgical action planning presents unique challenges that demand temporal, causal, and multimodal reasoning capabilities, areas poorly assessed by existing benchmarks. This task requires: (1) precise understanding of atomic tool-tissue interactions. These fine-grained and atomic actions that directly alter tissue states and form the universal building blocks of surgical workflows. (2) long-horizon reasoning to coordinate these atomic actions into coherent procedures. However, critical barriers persist, including the need to track instrument-tissue relationships, monitor surgical progress, and generalize across institutional variations. All compounded by the current scarcity of high-quality surgical action planning datasets.

The development of specialized datasets for atomic action planning is critical to advance this field. Such datasets must challenge models with: (1) Higher-order reasoning to infer causal relationships between actions. (2) Fine-grained visual distinction to recognize subtle tissue state changes. (3) Context-aware language understanding to align actions with procedural goals. By enabling rigorous evaluation of these capabilities, we aim to develop the surgical action planning datasets which will not only address current limitations in MLLM assessment but also accelerate the development of clinically relevant multimodal intelligence for real-world surgical applications, including enhanced intraoperative decision support and automated procedural workflow assistance.

The contributions of our work can be summarized as follows:

- We introduced surgical action planning task which generates future surgical action plans from visual inputs. This task requires precise atomic tool-tissue interaction understanding and long-horizon reasoning to bridge critical gaps in MLLM evaluation for clinical applications like intraoperative guidance and procedural automation.
- We introduced the SAP-Bench dataset spans a context duration of $1137.50 \pm 575.61s$ and includes $1,226$ action clips covering five surgical actions from 74 patients, with each clip lasting $68.66 \pm 115.99s$. It features $1,152$ extracted *"current frame"* as key temporal anchors for MLLM analysis, with 679 sourced from CholecT50 and 473 from HeiChole.
- We proposed an MLLM-based surgical action planning (MLLM-SAP) framework that generates *'next action'* recommendations. Using the *'current frame'*, a visual representation of the immediate tissue state, as input, the MLLM model processes natural language instructions after injecting the surgical domain knowledge. By holistically evaluating the scene understanding, process assessment, and safety considerations, the MLLM outputs *'next action'* proposals for intraoperative guidance.
- We evaluated the effectiveness of 7 state-of-the-art (SOTA) MLLM models, including OpenAI-o1, QwenVL2.5-Instruct-72B, Claude-3.5-Sonnet, GeminiPro2.5, Step-1o, and GLM-4v on our proposed SAP-Bench dataset.
- We engaged two board-certified surgeons to establish expert benchmarks for preferred next actions, while systematically evaluating prompt design components through ablation studies.

2 Related Work

General-purpose MLLM benchmarks Recent efforts to evaluate MLLMs have emphasized broad knowledge and reasoning across diverse domains, with benchmarks primarily focusing on retro-

spective tasks (e.g., recognition, perception) rather than proactive decision-making. For concept recognition, works like MM-Vet [25], LLaVA-Bench [9], and Open-VQA [28] identify key visual concepts such as objects, instances, and scenes. In action recognition, benchmarks such as MM-Bench [10], SEED-Bench [6], EQBEN [21], and Visual CoT [18] recognize actions performed by subjects. For attribute-based tasks, CV-Bench [19] and Q-Bench [22] assess the model's ability to recognize visual attributes (e.g., style, mood, quality), whereas object localization is addressed by MDVP-Bench [8] and VL-Checklist [29]. Spatial relationship understanding (e.g., "left of," "before") is benchmarked in VSR [9] and GQA [4], while object interaction, critical for real-world reasoning, is evaluated in SEED-Bench [6], VL-Checklist [29], ARO [27], and CODIS [12]. While these benchmarks have advanced general visual and commonsense reasoning, they remain inadequate for assessing procedural planning or domain-specific reasoning, particularly the surgical-specific proactive planning with tool-tissue interactions and long-horizon causal dynamics that our work targets. The application of MLLMs to sequential task planning has shown significant potential. These models combine visual-language understanding with sequential decision-making, enabling them to process environmental contexts, establish task objectives, and generate actionable plans. Their effectiveness in daily activity planning scenarios has been well-documented in recent studies [2, 3, 5].

Medical-specific MLLMs In the clinical domain, models such as Med-Flamingo [13] and Rad-DINO [16] demonstrate strong performance in diagnostic tasks (e.g., radiology report generation or medical image QA). However, these systems are tailored for passive observation (e.g., interpreting scans or notes) rather than active decision-making, such as surgical planning or intraoperative reasoning. While datasets like MedReason [23] introduce structured medical reasoning, they remain confined to diagnostic contexts, omitting the dynamic, tool-aware reasoning needed in surgery. Prior work in surgical AI has largely focused on retrospective analysis, such as phase recognition [1], instrument segmentation [24], and interaction detection [15]. These efforts improve the understanding of the surgical scene but fail to model higher-level cognitive processes, such as surgical procedure planning or decision-making during procedures. Recent initiatives like SurgRaw [11] aim to bridge this gap by capturing raw surgical workflows, but they lack explicit annotations for reasoning or long-horizon task decomposition. Our work unifies these perspectives by introducing a benchmark for surgical action planning, combining the multimodal breadth of general MLLM evaluations, the domain specificity of medical MLLMs, and the procedural rigor missing in existing surgical AI datasets.

3 Approach

3.1 Surgical action planning (SAP) task definition

SAP task breaks down intricate procedures into universal and fundamental actions and produces long-horizon sequential action plans from visual inputs, enabling the achievement of user-defined objectives. Specifically, the surgical action planner formulates an action plan $\mathcal{A} = \{a_1, \ldots, a_T\}$ by integrating two primary inputs: (1) a visual history $\mathcal{H} = \{v_1, \ldots, v_t\}$, encoding past observations as a sequence of video clips or frames, and (2) a goal specification G, provided as a natural language instruction (e.g., *"What's the next action in laparoscopic cholecystectomy"*). The planner generates a sequence of discrete actions $\{a_t\}_{t=1}^{T}$, where each $a_t \in \{1, \ldots, C\}$ belongs to a predefined set of C surgical actions, ensuring progression from the current state to the target goal within a T-step horizon.

3.2 SAP-Bench Dataset Benchmark

Source: Our SAP-Bench dataset is derived from three surgical video datasets: CholecT50 [15], and HeiChole [20], comprising 50, and 24 cholecystectomy procedures, respectively. A standard cholecystectomy consists of seven phases: (1) Preparation, (2) Calot triangle dissection, (3) Clipping and cutting, (4) Gallbladder dissection, (5) Gallbladder packing, (6) Cleaning and coagulation, and (7) Gallbladder retraction. For our study, we focus on processing video segments from phases 2–4 as the surgical action planning context, which include Calot triangle dissection, clipping and cutting, and gallbladder dissection, as these stages represent the most critical and technically demanding portions of the procedure, where precise anatomical manipulation and decision-making are paramount.

Manual action annotation and action clip extraction The action labels include aspiration, coagulation, dissection, tissue retraction, and vessel clipping. We build the annotation criteria of these

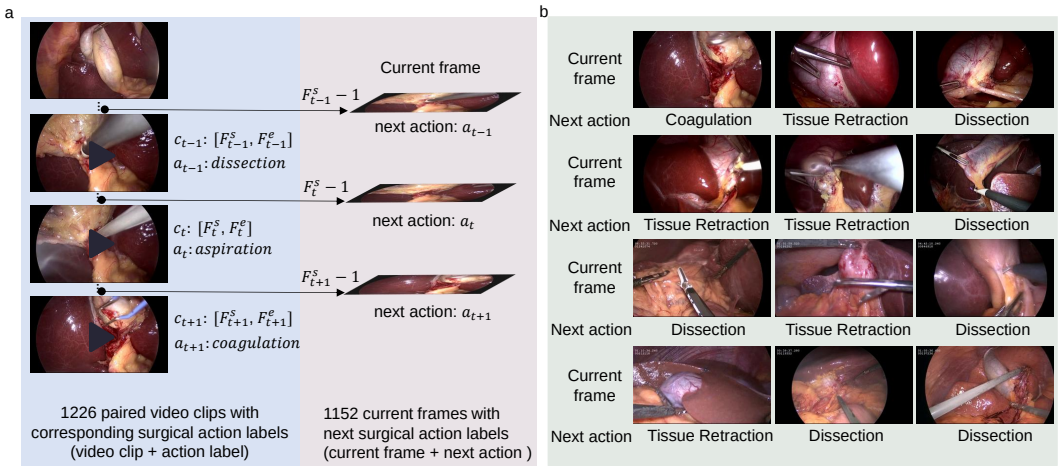

Figure 1: SAP-Bench Dataset. (a) We first annotate the action clips, recording both the action label a_{t+1} and the frame range $[F^s_{t+1}, F^e_{t+1}]$ for each. Then, we extract the frame immediately before the starting frame of each clip $F^s_{t+1} - 1$ as the *"current frame"* and assign the subsequent action label a_{t+1} as the *"next action"*. (b) Examples of current frames and their corresponding next actions.

5 surgical actions. *Aspiration:* removing fluids or tissue debris from the surgical site, typically through suction. *Coagulation:* applying thermal energy to promote hemostasis by denaturing proteins, forming a stable clot, and sealing tissue. *Dissection:* separating or cutting of tissue layers to expose underlying structures during surgery and access deeper anatomical layers. *Clipping:* applying surgical clamps to control bleeding or temporarily occlude blood vessels or tissue. *Tissue Retraction:* holding and manipulating tissues or organs aside to provide better visibility and access to the surgical site. Consecutive frames sharing identical action labels are grouped into action clips. To ensure data quality, we enforce strict selection criteria: (a) visual centrality: The target action must occupy the visual center to maintain context; (b) action purity: Each clip must contain exactly one distinguishable action. All action clips undergo a rigorous manual verification process to confirm label accuracy.

Dataset characteristics As shown in Table 1, our SAP-Bench dataset aggregates data from two surgical video datasets (i.e. CholecT50 and HeiChole), comprising 74 patients and $1,226$ action clips with their corresponding action label in total. The CholecT50 dataset contributes 50 patients with 729 clips, while HeiChole provides 24 patients with 497 clips. These $1,226$ action clips cover five surgical actions, as shown in Table 2. The dissection category dominates the collection with 597 instances (48.7% of total), averaging 112.32 ± 150.34 seconds per clip, contributing $67,056$ frames at 1 FPS. Tissue retraction appears most frequently after dissection (321 clips, 26.2%), though with notably shorter average duration ($20.65 \pm 19.84s$). Vessel clipping has 140 clips averaging 31.66 ± 30.21 seconds, coagulation has 110 clips, and aspiration has 58 clips.
Contextual video segments spanning from phase 2 to phase 4 have durations of $1,339.06 \pm 560.63s$ for CholecT50 and $717.58 \pm 325.32s$ for HeiChole. The duration of action clips measures $68.66 \pm 115.99s(overall)$, with CholecT50 averaging $91.84 \pm 142.77s$ and HeiChole averaging $34.65 \pm 36.61s$.
The current observation is defined as the *"current frame"* $F^s_{t+1} - 1$ immediately preceding the starting frame F^s_{t+1} of the subsequent action clip, where the clip spans frames $[F^s_{t+1}, F^e_{t+1}]$. The action label a_{t+1} of the subsequent action clip serves as the ground truth for *"next action"*. We extracted $1,152$ *"current frames"* as key temporal anchors for MLLM analysis, comprising 679 from CholecT50 and 473 from HeiChole. Each *"current frame"* has an assigned *"next action"* label.

Table 1: Dataset summary: number of patients, total clips, context duration per video (avg $\pm$ std) [s], action clip duration (avg $\pm$ std) [s], 1 FPS frames count, and current frames.

Source Dataset	# Patients	# Clips	Context Duration [s]	Clip Duration [s]	1 FPS Frame Count	# Current Frame
CholecT50	50	729	1339.06 $\pm$ 560.63	91.84 $\pm$ 142.77	66 953	679
HeiChole	24	497	717.58 $\pm$ 325.32	34.65 $\pm$ 36.61	17 222	473
Overall	74	1226	1137.50 $\pm$ 575.61	68.66 $\pm$ 115.99	84 175	1152

Table 2: action clip counts, duration statistics (mean ± SD), and 1 FPS frames count by dataset and overall.

Action	CholecT50			HeiChole			Overall		
	Count	Duration [s]	1 FPS Frame Count	Count	Duration [s]	1 FPS Frame Count	Count	Duration [s]	1 FPS Frame Count
Aspiration	39	36.00 ± 47.60	1404	19	37.05 ± 20.05	704	58	36.34 ± 40.69	2108
Coagulation	89	40.62 ± 65.79	3615	21	15.95 ± 15.11	335	110	35.91 ± 60.33	3950
Dissection	298	179.75 ± 185.51	53565	299	45.12 ± 42.24	13491	597	112.32 ± 150.34	67056
Tissue Retraction	232	22.50 ± 21.35	5221	89	15.81 ± 14.13	1407	321	20.65 ± 19.84	6628
Vessel Clipping	71	44.34 ± 35.91	3148	69	18.62 ± 13.76	1285	140	31.66 ± 30.21	4433

3.3 MLLM-based surgical action planning (MLLM-SAP) framework

Given the current capabilities of MLLMs in processing images, we employ only the current frame to represent the current observation $\mathcal{O}$ as visual input rather than video sequences. The MLLM processes the current observation $\mathcal{O}$ and prompts to generate the predicted next action $\mathcal{A}$. This design choice is motivated by: (1) MLLMs' demonstrated proficiency in single-image understanding, (2) computational efficiency considerations, and (3) the need for real-time processing in our surgical application.

$$\mathcal{A} = \text{MLLM}(\mathcal{O}, \textit{Prompts}) \tag{1}$$

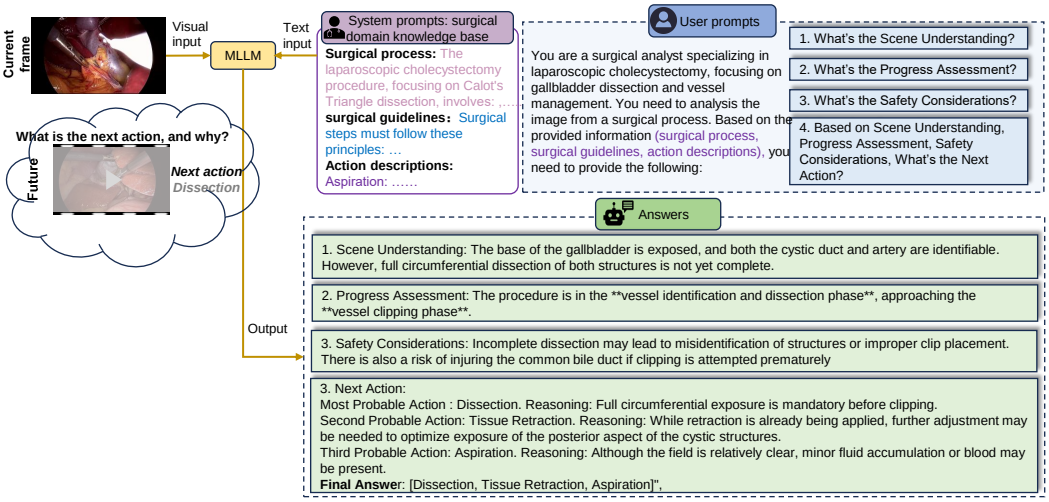

Figure 2: Our MLLM framework produces surgical action plans. Given the *"current frame"* as the observational input, which captures the latest tissue state, the MLLM processes both the system prompts and user-provided textual instructions. Based on integrated analysis of scene understanding, procedural progress, and safety considerations, the MMLLM model recommends the *"next action"*.

Prompts design for generating action plans Medical reasoning tasks demand rigorous logical processes. Specifically, we need a model capable of (1) decomposing complex problems into coherent reasoning steps, and (2) adhering to established medical guidelines to ensure professional, accurate responses supported by evidence-based rationales. Unlike mathematical problems that follow clear, stepwise solutions, medical question-answering involves navigating specialized terminology and extracting critical clues from complex clinical information to reach correct diagnoses, a significantly more challenging reasoning process. Therefore, our prompt engineering framework consists of two key components: **system prompts** and **user prompts**. The **system prompts** incorporate a structured surgical knowledge base that provides the MLLM with domain-specific information, including *surgical process*, *surgical guidelines*, and *action description* (see Figure 2). *Surgical process* defines the standardized sequence of steps and procedures performed during an operation. *Safety protocol* establishes rules and measures to minimize risks during medical interventions. *Action description* explains individual actions performed by surgeons. The **user prompts** capture real-time decision-making aspects and guide the system's responses with specific queries, including *scene understanding*, *progress judgment*, *safety considerations*, and *ready-to-execute actions*. Specifically,

scene understanding analyzes visual and contextual elements, such as key structures and spatial relationships, to establish the current state. *Progress judgment* dynamically tracks task advancement against the planned workflow, enabling real-time adjustments. *Safety considerations* continuously evaluate risks to prioritize harm-minimizing action. *Ready-to-execute actions* provides three recommended next actions. For each action, provide a rationale explaining why it is ranked in that order.

4 Experiment

GPT-4o, QwenVL2.5-Instruct-72B, Claude-3.5-Sonnet, GeminiPro2.5, Step-1o, and GLM-4v are selected as baseline MLLM models due to their support for vision inputs and their strong capabilities in image understanding and reasoning tasks. All Experiment were performed on 8 NVIDIA A800 GPUs. We adopt the following evaluation metrics:

Sample-S: For a prediction to be considered correct under the standard Sample-level accuracy (Sample-S), the model's predicted next action $\hat{a}_i$ must precisely match the ground truth action a_i at every timestep. The Top-2 and Top-3 metrics provide more lenient evaluation criteria. Here, a prediction is counted as correct if the true action a_i appears anywhere within the model's top two or three most likely predictions, respectively.

Video-S: To evaluate model generalization across complete surgical procedures, we compute video-level (i.e., patient-level) accuracy by aggregating sample-wise predictions. For each patient case, we first determine the Sample-S accuracy at every timestep, then average these values across the entire procedure. This provides a comprehensive view of model performance at the individual surgery level rather than isolated samples.

Sample-R: To better reflect the temporal variability inherent in surgical workflows, we introduce a relaxed accuracy metric. A prediction $\hat{a}_i$ is considered valid if it matches either the current ground truth action a_i or the immediately following action a_{i+1}. This +1-step tolerance ($\hat{a}_i \in \{a_i, a_{i+1}\}$) accommodates the natural temporal flexibility required during actual surgical procedures, where certain steps may be safely reordered without clinical consequence.

Video-R: To provide a holistic assessment of model performance at the patient level while accommodating the inherent temporal variability present in real-world surgical workflows, we aggregate predictions at the video-level (i.e., patient-level). For each video, we compute sample-wise accuracy using the relaxed criterion (Sample-R), then derive a unified performance score by averaging these values throughout the entire procedure.

4.1 Results

Our evaluation of 7 state-of-the-art MLLMs (OpenAI-o1, GPT-4o, QwenVL2.5-72B, Claude-3.5-Sonnet, GeminiPro2.5, Step-1o, and GLM-4v) across CholecT50 and HeiChole reveals critical differences in surgical reasoning capabilities from the sample level and video level under both Standard (S) and Relaxed (R) conditions (see Table 3 and Figure 3). Key findings include:

1. Performance hierarchy and model strengths. OpenAI-o1, leveraging reasoning ability, achieves the best Top-1 Sample-S and Sample-R on Cholec50, and ranks second in Sample-S and first in Sample-R on HeiChole, demonstrating strong performance. GPT-4o consistently leads in Top-1 Sample-S accuracy under Standard conditions (e.g., 34.61% on Cholec50 and 59.20% on HeiChole), demonstrating good generalization. GLM-4v shows the lowest Top-1 Sample–S but the highest Top-3 Sample–S, suggesting strong retrieval-augmented reasoning but weaker precision.

2. Dataset-specific challenges. CholecT50 proves more challenging than HeiChole, with all models showing significantly lower Top-1 scores (e.g., 28.87% on CholecT50 for Claude-3.5-Sonnet vs. 46.30% on HeiChole). This gap narrows in Top-3 metrics, implying higher ambiguity in fine-grained surgical step classification.

3. Impact of evaluation rigor. Transitioning from Standard (S) to Relaxed (R) conditions universally boosts performance, with Top-1 Sample-S gains exceeding 20% (e.g., GPT-4o jumps from 34.61% to 67.41% on Cholec50). This highlights the sensitivity of MLLMs to strict surgical benchmarks. Video-based evaluation (Video-S and Video-R) shows better performance over Sample-level metrics for most models (e.g., Step-1o's 71.47% Top-1 Video-R vs. 67.25% Top-1 Sample-R on CholecT50).

4. Model limitations. GLM-4v and Claude-3.5-Sonnet struggles with surgical action planning task, scoring lowest on Top-1 Sample-S and Top-3 Sample-S for Cholec50, respectively.

Figure 3 displays the model's predicted textual responses to user prompts, covering *scene understanding*, *progress assessment*, *safety considerations*, and *ready-to-execute actions*. Correct responses are highlighted in green, while errors are marked in pink. The analysis focuses on a surgical procedure involving the dissection of Calot's Triangle, with clear identification of key anatomical structures such as the cystic duct and artery. It evaluates the necessity for further dissection while emphasizing procedural safety and optimal visibility.

Table 3: Comparative performance on CholecT50 and HeiChole datasets evaluated at both sample-level (per-frame) and video-level (per-patient) granularity under Standard (exact-match) and Relaxed (+1-step tolerance) conditions. **Bold** values indicate the best performance, while underlined values denote the poorest results for each metric.

Dataset	Model	Sample-S			Video-S			Sample-R			Video-R		
		Top 1	Top 2	Top 3	Top 1	Top 2	Top 3	Top 1	Top 2	Top 3	Top 1	Top 2	Top 3
CholecT50	OpenAI-o1	**36.82**	44.04	46.69	39.42	45.57	48.93	**69.16**	78.54	79.33	74.01	81.61	82.15
	GPT-4o	34.61	**64.21**	77.76	35.86	62.48	75.85	67.41	**92.21**	**97.62**	69.82	**92.75**	97.53
	QwenVL2.5-Instruct-72B	29.01	55.82	73.93	31.01	55.83	71.61	58.51	85.85	96.50	61.86	86.08	94.70
	Claude-3.5-Sonnet	28.87	48.31	57.44	30.87	49.62	57.82	57.23	78.38	83.78	59.23	80.07	84.58
	GeminiPro2.5	28.87	58.03	77.47	30.42	56.49	75.13	51.99	84.58	95.55	51.12	82.15	93.38
	Step-1o	34.46	53.76	69.37	**35.93**	55.59	69.46	67.25	85.21	95.07	**71.47**	87.89	95.88
	GLM-4v	18.02	51.70	**81.09**	21.47	55.96	**81.74**	36.84	86.60	96.81	41.75	89.41	**97.74**
HeiChole	OpenAI-o1	57.29	63.85	64.06	57.35	64.02	64.28	**76.61**	84.41	84.41	76.94	84.64	84.64
	GPT-4o	**59.20**	74.42	83.09	**59.00**	74.73	83.46	**76.61**	90.87	94.65	**76.46**	90.59	94.29
	QwenVL2.5-Instruct-72B	48.63	74.84	**86.05**	48.39	74.60	**86.23**	63.92	89.76	95.32	63.60	89.66	95.23
	Claude-3.5-Sonnet	46.30	64.69	66.38	45.42	64.81	66.58	65.26	82.85	83.30	64.27	82.41	82.76
	GeminiPro2.5	46.30	68.29	79.07	44.90	67.63	78.35	64.81	82.85	90.20	63.41	81.47	89.03
	Step-1o	53.91	68.50	76.74	53.63	68.59	76.68	71.94	86.41	90.65	71.73	86.78	90.49
	GLM-4v	29.66	**76.69**	86.02	29.58	**77.22**	86.12	47.77	**93.97**	**97.10**	48.17	**94.09**	**96.98**

4.2 Human evaluation: clinical variability in surgical decision-making

Surgical workflows exhibit inherent variability due to: (i) Skill-dependent factors: Surgeon experience level (e.g., resident vs. attending) (ii) Style variations: Individual operative preferences (e.g., dissection techniques) (iii) Contextual adaptability: Real-time adjustments based on tissue conditions This variability implies that the observed next action in any surgical video represents just one possible valid approach, not necessarily a unique optimal solution.

To establish expert-validated performance benchmarks, we engaged two board-certified surgeons (A and B) to provide their preferred *"next action"*. From the CholecT50 dataset, we selected 64 samples across 50 surgical videos, asking each surgeon to indicate their preferred next action for every sample. For these 64 samples, we evaluate MLLM models' predictions against four distinct *"next action"* ground truth references: (1) *GT from video*: The actual *"next action"* performed in the surgical video (the ground truth from the original surgeon's demonstration). (2) *Surgeon A*: The preferred *"next action"* suggested by expert surgeons A. (3) *Surgeon B*: The preferred *"next action"* suggested by expert surgeons B. (4) *Surgeon (A or B)*: A match is counted if the model's prediction aligns with either surgeon A or B's preferred *"next action"*, representing broader expert consensus.

As shown in Figure 4, we assess GPT-4o's performance using Top-k Sample-S accuracy ($k \in 1, 2, 3$), measuring alignment with: (1) individual surgeon preferences (The surgeon who performed the surgery vs. the Surgeon A vs. the Surgeon B), and (2) decisions combining two experts judgments. This dual evaluation approach captures both regional surgical practice variations and general expert consensus. GPT-4o performs best with surgeon B consensus (38.30% Top-1) and combined evaluations (58.51% Top-1). Particularly telling is the average performance boost when evaluating against combined surgeon preferences (HK or SG) versus individual assessments.

4.3 Ablation study

We conduct a systematic ablation study to analyze the impact of different textual components in our prompt design, focusing on two key elements: system prompts and user prompts (see Table 4). The **system prompts** include *surgical process*, *surgical guidelines*, and *action description*. The **user prompts** include *scene understanding*, *progress judgment*, *safety considerations*, and *ready-to-execute actions*. We evaluate the following variations: (1) w/o SP: Complete removal of all **S**ystem **P**rompts (SP) while retaining user prompts. (2) w. OA: User prompts restricted to **O**nly *ready-to-execute **A**ctions* (OA) (excluding *scene understanding*, *progress judgment*, and *safety considerations*),

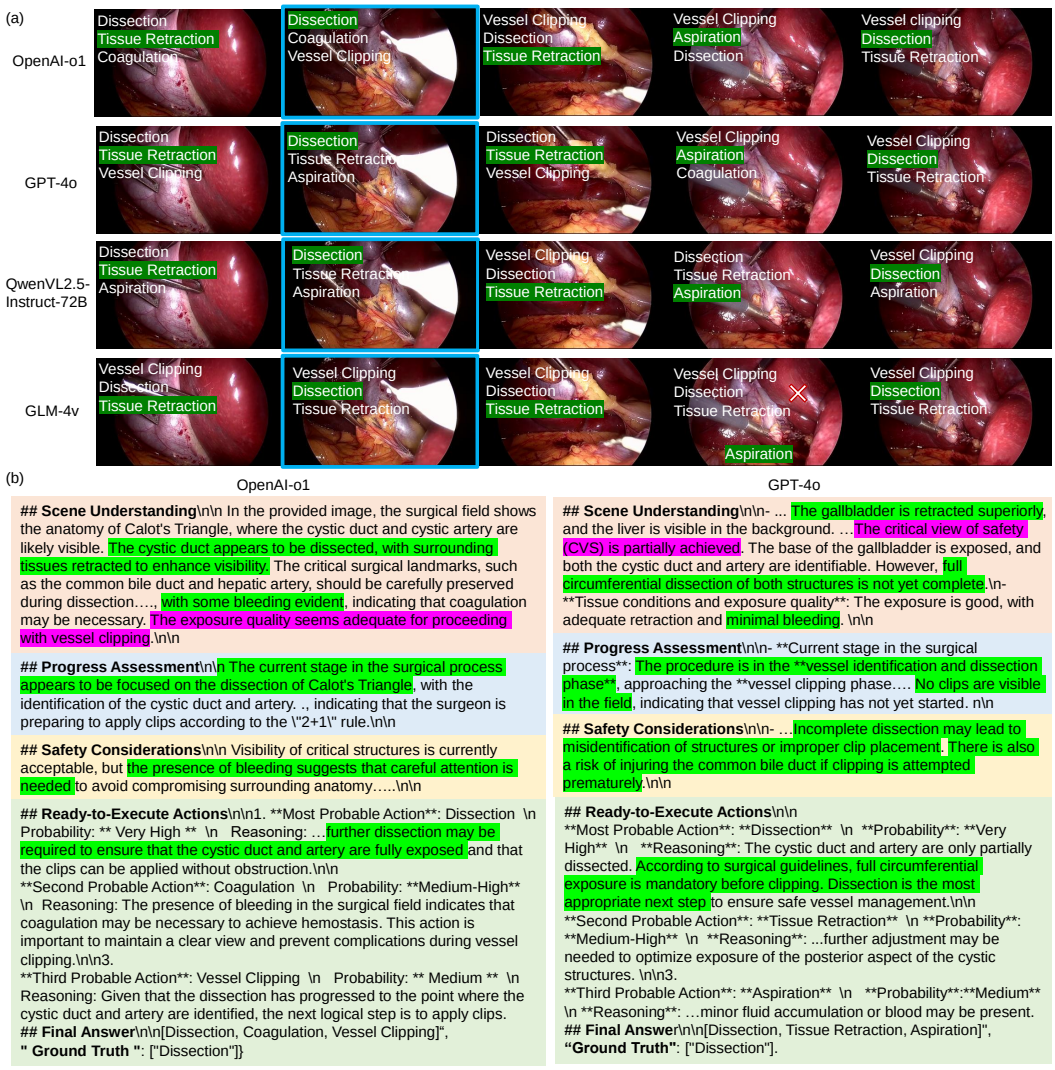

Figure 3: Visualization of results. (a) Action planning predictions: White text displays the top 3 predicted future actions (ranked in order), with $\times$ marking incorrect predictions. Ground truth actions are highlighted in green. (b) In the case of the sample highlighted by the blue bounding box in (a), the MLLMs generates textual predictions that predict the next action. The text highlighted in green indicates correct responses, while pink highlights denote errors.

preserving system prompts. We use Δ to represent the performance difference (in percentage points) between an ablated model variant and its base version.

Ablation study on system prompts We quantitatively evaluate the impact of system prompts by comparing model performance with and without surgical knowledge injection. The removal of system prompts (w/o SP) consistently degrades performance across most model-dataset combinations, with GPT-4o showing the largest performance drop ($\Delta = -8.85$ on HeiChole Video-S). This underscores their critical role in maintaining contextual understanding, particularly for complex surgical scenarios requiring procedural knowledge and safety constraints. The consistent performance drop across both datasets confirms the necessity of domain-specific knowledge injection and demonstrates the generalizability of prompt engineering for surgical MLLMs.

Ablation study on user prompts The only ready-to-execute actions user prompts (w. OA) produce divergent effects. While GPT-4o suffers significant degradation in w. OA mode ($\Delta = -8.69$ on CholecT50 Sample-S, and $\Delta = -15.86$ on HeiChole Sample-S). GeminiPro2.5 benefits from this

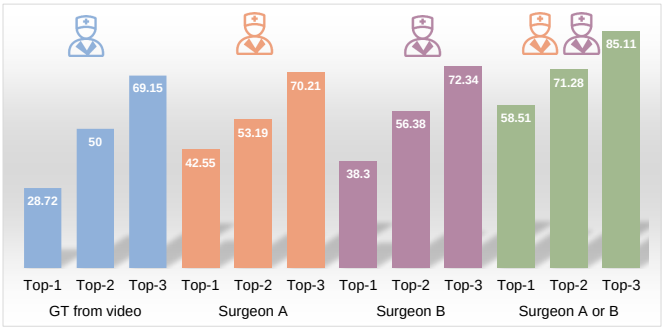

Figure 4: Model performance evaluation against four ground truth references, including original surgery, and surgeon preferences (A, B, or either) using Top-k Sample-S accuracy ($k \in 1, 2, 3$).

simplification ($\Delta = +6.97$ on HeiChole Sample-S), suggesting fundamental differences in how models process instructional context. QwenVL suffers the most severe degradation ($\Delta = -21.36$ on HeiChole Sample-S) These findings suggest that while OA filtering reduces hallucination risks, it disproportionately affects models with stronger reasoning but weaker surgical-action grounding.

Table 4: Performance comparison (Top-1 accuracy Δ) between ablation variants and base models across datasets. Ablation variants include system prompt removal (w/o SP) and only ready-to-execute actions user prompt (w. OA). Δ represents the performance difference (in percentage points) between an ablated model variant and its base version.

	CholecT50		HeiChole	
Model	**Sample-SΔ**	**Video-SΔ**	**Sample-SΔ**	**Video-SΔ**
w/o SP				
GPT-4o	-4.12	-1.87	-6.77	-6.33
GeminiPro2.5	+2.80	+1.33	-0.22	-1.15
QwenVL	-5.15	-4.78	-11.63	-11.30
w. OA				
GPT-4o	-8.69	-8.52	-15.86	-14.85
GeminiPro2.5	+5.01	+3.11	+6.97	+6.34
QwenVL	-2.06	-2.45	-21.36	-21.97

5 Conclusion

Effective evaluation is essential for advancing MLLM research, particularly in surgical action planning (SAP), a task requiring precise, multimodal reasoning to generate future action sequences from visual inputs. Therefore, we introduce SAP-Bench benchmark, a large-scale dataset derived from 74 cholecystectomy procedures, featuring 1,226 clinically validated action clips and 1,152 *current frames* paired with *next actions* for multimodal analysis. We also propose MLLM-SAP, a framework that leverages MLLMs enhanced with surgical knowledge to generate actionable *next action* recommendations. Evaluating seven leading MLLMs (e.g., GPT-4o, Claude-3.5-Sonnet, QwenVL2.5-72B), we identify significant gaps in surgical action prediction. To ground our evaluation in clinical reality, we collaborated with two board-certified surgeons to establish expert benchmarks and conducted ablation studies to evaluate the impact of prompt design components in intraoperative decision-making. **Limitations:** Our current framework has two main limitations: (1) we have not employed reinforcement learning to validate model effectiveness, and (2) the MLLM-SAP architecture does not incorporate Chain-of-Thought (CoT) reasoning mechanisms. **Future works:** Beyond performance metrics, assessing the trustworthiness of MLLMs is vital to ensure their reliability in high-stakes domains such as healthcare systems, where errors can have serious consequences. Furthermore, evaluating MLLMs across a broad spectrum of downstream applications helps verify their adaptability, ensuring they can meet the nuanced requirements of real-world deployment.

References

[1] Ayobi, N., Rodríguez, S., Pérez, A., Hernández, I., Aparicio, N., Dessevres, E., Peña, S., Santander, J., Caicedo, J.I., Fernández, N., Arbeláez, P.: Pixel-wise recognition for holistic surgical scene understanding. arXiv (2024), https://arxiv.org/abs/2401.11174

[2] Chen, Y., Ge, Y., Ge, Y., Ding, M., Li, B., Wang, R., Xu, R., Shan, Y., Liu, X.: Egoplan-bench: Benchmarking multimodal large language models for human-level planning. arXiv preprint arXiv:2312.06722 (2023)

[3] Huang, D., Hilliges, O., Van Gool, L., Wang, X.: Palm: Predicting actions through language models @ ego4d long-term action anticipation challenge. arXiv preprint arXiv:2306.16545 (2023)

[4] Hudson, D.A., Manning, C.D.: Gqa: A new dataset for real-world visual reasoning and compositional question answering. In: Proceedings of the IEEE/CVF conference on computer vision and pattern recognition. pp. 6700–6709 (2019)

[5] Kim, S., Huang, D., Xian, Y., Hilliges, O., Van Gool, L., Wang, X.: Palm: Predicting actions through language models. In: European Conference on Computer Vision. pp. 140–158. Springer (2024)

[6] Li, B., Ge, Y., Ge, Y., Wang, G., Wang, R., Zhang, R., Shan, Y.: Seed-bench: Benchmarking multimodal large language models. In: Proceedings of the IEEE/CVF Conference on Computer Vision and Pattern Recognition. pp. 13299–13308 (2024)

[7] Li, B., Wang, R., Wang, G., Ge, Y., Ge, Y., Shan, Y.: Seed-bench: Benchmarking multimodal llms with generative comprehension. arXiv preprint arXiv:2307.16125 (2023)

[8] Lin, W., Wei, X., An, R., Gao, P., Zou, B., Luo, Y., Huang, S., Zhang, S., Li, H.: Draw-and-understand: Leveraging visual prompts to enable mllms to comprehend what you want. arXiv preprint arXiv:2403.20271 (2024)

[9] Liu, F., Emerson, G., Collier, N.: Visual spatial reasoning. Transactions of the Association for Computational Linguistics **11**, 635–651 (2023)

[10] Liu, Y., Duan, H., Zhang, Y., Li, B., Zhang, S., Zhao, W., Yuan, Y., Wang, J., He, C., Liu, Z., et al.: Mmbench: Is your multi-modal model an all-around player? In: European conference on computer vision. pp. 216–233. Springer (2024)

[11] Low, C.H., Wang, Z., Zhang, T., Zeng, Z., Zhuo, Z., Mazomenos, E.B., Jin, Y.: Surgraw: Multi-agent workflow with chain-of-thought reasoning for surgical intelligence. arXiv preprint arXiv:2503.10265 (2025)

[12] Luo, F., Chen, C., Wan, Z., Kang, Z., Yan, Q., Li, Y., Wang, X., Wang, S., Wang, Z., Mi, X., et al.: Codis: Benchmarking context-dependent visual comprehension for multimodal large language models. arXiv preprint arXiv:2402.13607 (2024)

[13] Moor, M., Huang, Q., Wu, S., Yasunaga, M., Dalmia, Y., Leskovec, J., Zakka, C., Reis, E.P., Rajpurkar, P.: Med-flamingo: a multimodal medical few-shot learner. In: Machine Learning for Health (ML4H). pp. 353–367. PMLR (2023)

[14] Nie, J., Zhang, G., An, W., Tan, Y.P., Kot, A.C., Lu, S.: Mmrel: A relation understanding dataset and benchmark in the mllm era. arXiv preprint arXiv:2406.09121 (2024)

[15] Nwoye, C.I., Yu, T., Gonzalez, C., Seeliger, B., Mascagni, P., Mutter, D., Marescaux, J., Padoy, N.: Rendezvous: Attention mechanisms for the recognition of surgical action triplets in endoscopic videos. Medical Image Analysis **78**, 102433 (2022)

[16] Pérez-García, F., Sharma, H., Bond-Taylor, S., Bouzid, K., Salvatelli, V., Ilse, M., Bannur, S., Castro, D.C., Schwaighofer, A., Lungren, M.P., et al.: Rad-dino: Exploring scalable medical image encoders beyond text supervision. arXiv preprint arXiv:2401.10815 (2024)

[17] Saikh, T., Ghosal, T., Mittal, A., Ekbal, A., Bhattacharyya, P.: Scienceqa: A novel resource for question answering on scholarly articles. International Journal on Digital Libraries **23**(3), 289–301 (2022)

[18] Shao, H., Qian, S., Xiao, H., Song, G., Zong, Z., Wang, L., Liu, Y., Li, H.: Visual cot: Unleashing chain-of-thought reasoning in multi-modal language models. arXiv e-prints pp. arXiv–2403 (2024)

[19] Tong, P., Brown, E., Wu, P., Woo, S., IYER, A.J.V., Akula, S.C., Yang, S., Yang, J., Middepogu, M., Wang, Z., et al.: Cambrian-1: A fully open, vision-centric exploration of multimodal llms. Advances in Neural Information Processing Systems **37**, 87310–87356 (2024)

[20] Wagner, M., Müller-Stich, B.P., Kisilenko, A., Tran, D., Heger, P., Mündermann, L., Lubotsky, D.M., Müller, B., Davitashvili, T., Capek, M., et al.: Comparative validation of machine learning algorithms for surgical workflow and skill analysis with the heichole benchmark. Medical Image Analysis **86**, 102770 (2023)

[21] Wang, T., Lin, K., Li, L., Lin, C.C., Yang, Z., Zhang, H., Liu, Z., Wang, L.: Equivariant similarity for vision-language foundation models. In: Proceedings of the IEEE/CVF International Conference on Computer Vision. pp. 11998–12008 (2023)

[22] Wu, H., Zhang, Z., Zhang, E., Chen, C., Liao, L., Wang, A., Li, C., Sun, W., Yan, Q., Zhai, G., et al.: Q-bench: A benchmark for general-purpose foundation models on low-level vision. arXiv preprint arXiv:2309.14181 (2023)

[23] Wu, J., Deng, W., Li, X., Liu, S., Mi, T., Peng, Y., Xu, Z., Liu, Y., Cho, H., Choi, C.I., et al.: Medreason: Eliciting factual medical reasoning steps in llms via knowledge graphs. arXiv preprint arXiv:2504.00993 (2025)

[24] Xu, M., Islam, M., Bai, L., Ren, H.: Privacy-preserving synthetic continual semantic segmentation for robotic surgery. IEEE transactions on medical imaging (2024)

[25] Yu, W., Yang, Z., Li, L., Wang, J., Lin, K., Liu, Z., Wang, X., Wang, L.: Mm-vet: Evaluating large multimodal models for integrated capabilities. arXiv preprint arXiv:2308.02490 (2023)

[26] Yue, X., Ni, Y., Zhang, K., Zheng, T., Liu, R., Zhang, G., Stevens, S., Jiang, D., Ren, W., Sun, Y., et al.: Mmmu: A massive multi-discipline multimodal understanding and reasoning benchmark for expert agi. In: Proceedings of the IEEE/CVF Conference on Computer Vision and Pattern Recognition. pp. 9556–9567 (2024)

[27] Yuksekgonul, M., Bianchi, F., Kalluri, P., Jurafsky, D., Zou, J.: When and why vision-language models behave like bags-of-words, and what to do about it? arXiv preprint arXiv:2210.01936 (2022)

[28] Zeng, Y., Zhang, H., Zheng, J., Xia, J., Wei, G., Wei, Y., Zhang, Y., Kong, T., Song, R.: What matters in training a gpt4-style language model with multimodal inputs? In: Proceedings of the 2024 Conference of the North American Chapter of the Association for Computational Linguistics: Human Language Technologies (Volume 1: Long Papers). pp. 7930–7957 (2024)

[29] Zhao, T., Zhang, T., Zhu, M., Shen, H., Lee, K., Lu, X., Yin, J.: Vl-checklist: Evaluating pre-trained vision-language models with objects, attributes and relations. arXiv preprint arXiv:2207.00221 (2022)